Nuclear effects in leading neutron production

B. Z. Kopeliovich, I. K. Potashnikova, and Iván Schmidt

Departamento de Física, Universidad Técnica Federico Santa María; and
Centro Científico-Tecnológico de Valparaíso; Casilla 110-V, Valparaíso, Chile

Absorptive corrections, known to suppress proton-neutron transitions with large fractional momentum $z \to 1$ in pp collisions, become dramatically strong on a nuclear target, and push the partial cross sections of leading neutron production to the very periphery of the nucleus. The mechanism of π-a_1 interference, which successfully explains the observed single-spin asymmetry in polarized $pp \to nX$, is extended to collisions of polarized protons with nuclei. Corrected for nuclear effects, it explains the observed single-spin azimuthal asymmetry of neutrons, produced in inelastic events, where the nucleus violently breaks up. The single-spin asymmetry is found to be negative and nearly A-independent.

I. WHY NEUTRON PRODUCTION?

The process $p + p(A) \to n + X$, with a large fractional light-cone momentum $z = p_n^+/p_p^+$ of neutrons produced in the proton beam direction, is known to be related to the iso-vector Reggeons (π, ρ, a_2, a_1, etc.) [1], as is illustrated in figure 1, where the amplitude, squared and summed over the final states X (at a fixed invariant mass M_X), is expressed via the Reggeon-proton total cross section at the c.m. energy M_X.
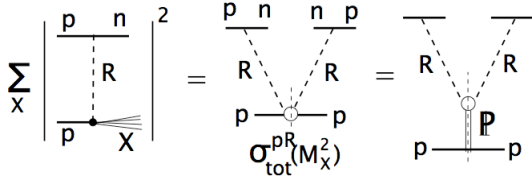

FIG. 1: Graphical relation between the cross section of neutron production and the total Reggeon-proton cross section, which at large M_X^2 is dominated by the Pomeron.

At high energies of colliders (RHIC, LHC) $M_X^2 = s(1-z)$ is so large (except of the inaccessibly small $1-z$), that the cross section $\sigma_{tot}^{pR}(M_X^2)$ is dominated by the Pomeron exchange, as is illustrated in figure 1.

The couplings of iso-vector Reggeons with natural parity (ρ, a_2) to the proton are known to be predominantly spin-flip [2], so they can be neglected, because we are interested here in small transverse momenta of neutrons, $p_T \to 0$. Only unnatural parity Reggeons (π, a_1), having large spin non-flip couplings contribute in the forward direction.

II. PROTON-TO-NEUTRON TRANSITION IN THE VICINITY OF PION POLE

Pions are known to have a large coupling with nucleons, so the pion exchange is important in the processes with isospin flip, like $p \to n$. Measurements with polarized proton beams supply more detailed information about the interaction dynamic.

The pion term in the cross section of neutron production reads [1],

$$z \left. \frac{d\sigma^B(pp \to nX)}{dz\, dq_T^2} \right|_\pi = f_{\pi/p}(z, q_T, q_L)\, \sigma_{tot}^{\pi^+ p}(s'), \quad (1)$$

where $s' = M_X^2$; and superscript B means that this is the Born approximation, ignoring absorptive corrections. $f_{\pi/p}(z, q_T, q_L)$ is the pion flux in the proton, having the form,

$$
\begin{aligned}
f_{\pi/p}(z, q_T, q_L) &= |t|\, G_{\pi^+ pn}^2(t)\, |\eta_\pi(t)|^2 \left(\frac{\alpha'_\pi}{8} \right)^2 \\
&\times (1-z)^{1-2\alpha_\pi(t)}.
\end{aligned}
\quad (2)
$$

Here q_T is the neutron transverse momentum; $q_L = m_N(1-z)/\sqrt{z}$; $-t = q_L^2 + q_T^2/z$; and $G_{\pi^+ pn}(t)$ is the effective π-N vertex function [1, 3].

The amplitude of the process includes both non-flip and spin-flip terms [1, 14],

$$A_{p\to n}^B(\vec{q}, z) = \bar{\xi}_n \left[\sigma_3\, q_L + \frac{1}{\sqrt{z}} \vec{\sigma} \cdot \vec{q}_T \right] \xi_p\, \phi^B(q_T, z), \quad (3)$$

The procedure of inclusion of the absorptive corrections on the amplitude level was developed in [1, 4]. First, the amplitude (3) is Fourier transformed to impact parameter representation, where the absorptive effect is just a multiplicative suppression factor. Then the absorption corrected amplitude is Fourier transformed back to momentum representation. The effects of absorption turn out to be quite strong, it about twice reduces the neutron production cross section, and affects differently the non-flip and spin-flip terms in the amplitude. Here we skip the derivation, which is too lengthy and is described in detail in [1, 4, 5].

III. LEADING NEUTRONS FROM pA COLLISIONS

Being close to the pion pole, we treat the vertex $\pi + p \rightarrow X$ in figure 1 as the pion-proton interaction amplitude. Squaring it, we get in (1) the pion-proton total cross section. In the case of a nuclear target we should replace the proton by a nucleus and get $\sigma_{tot}^{\pi A}(M_X^2)$. The latter gets contributions from different channels, which can be classified as inelastic and diffractive interactions. The former corresponds to multiparticles production filling the rapidity interval between the colliding pion and nucleus; while the latter corresponds to rapidity gap events. The corresponding cross sections can be evaluated within models as is described below.

The recent measurements of forward neutrons in the PHENIX experiment was supplemented by the Beam-Beam Counters (BBC), detecting charged particles in two pseudo-rapidity intervals $3.0 < |\eta| < 3.9$. The results of measurements of forward neutrons are presented for different samples of events:
(i) inclusive neutron production, with BBC switched off.
(ii) Neutrons accompanied with multi-particle production (one or both BBCs are fired), can be associated with inelastic π-A collisions;
(iii) If both BBC are vetoed, a large contribution of diffractive interactions might be expected.

Notice that such a correlation with BBC activities and related processes should not be taken literally, and comparison with theoretical predictions should be done with precaution. Further experimental studies employing Monte-Carlo simulations are required.

A. Glauber model

A natural extension of equation (1) to nuclear targets has the form,

$$\frac{d\sigma(pA \rightarrow nX)}{d\ln(z)dq_T^2 d^2 b_A} = f_{\pi/p}(z, q_T)\frac{d\sigma_{tot}^{\pi A}(M_X^2)}{d^2 b_A} S_{NA}(b_A), \quad (4)$$

where b_A is the impact parameter of pA collision; $S_{NA}(b_A)$ is the additional nuclear absorption factor described below.

This expression can be interpreted as interaction of the projectile Fock component $|\pi^+ n\rangle$ with the target, sharing the proton light-cone momentum in fractions z and $(1-z)$ respectively. While the pion interacts inelastically with the target, the spectator neutron has to remain intact, i.e. has to survive propagation through the nucleus.

The partial total pion-nucleus cross section in equation (4) can be evaluated in the Glauber approximation,

$$\frac{\sigma_{tot}^{\pi A}(M_X^2)}{d^2 b_A}\bigg|_{Gl} \approx 2\left[1 - e^{-\frac{1}{2}\sigma_{tot}^{\pi N}(M_X^2)T_A(b_A)}\right], \quad (5)$$

where $T_A(b_A) = \int_{-\infty}^{\infty} d\zeta\, \rho_A(b_A, \zeta)$, is the nuclear thickness function; $\rho_A(b_A, \zeta)$ is the nuclear density. Notice that for numerical calculations we use here and in

what follows more accurate form, replacing $e^{-\frac{1}{2}\sigma_{tot}^{\pi N}T_A} \Rightarrow [1 - \sigma_{tot}^{\pi N}T_A/2A]^A$.

Correspondingly, the neutron survival factor in (4) reads,

$$\begin{aligned}S_{NA}(b_A)\big|_{Gl} &\approx \frac{e^{-\sigma_{in}^{nN}(zs)T_A(b_A)} - e^{-\sigma_{in}^{pN}(s)T_A(b_A)}}{T_A(b_A)[\sigma_{in}^{pN}(s) - \sigma_{in}^{nN}(zs)]} \\ &\approx e^{-\sigma_{in}^{NN}(s)T_A(b_A)}. \quad (6)\end{aligned}$$

If BBC are vetoed, the nucleus quite probably remains intact or decays into fragments without particle production. Then instead of the total πA cross section one should use in (4) diffractive cross section related to elastic, $\pi A \rightarrow \pi A$, and quasielastic $\pi A \rightarrow \pi A^*$, channels. The corresponding cross section has the form [8, 9],

$$\begin{aligned}\frac{\sigma_{diff}^{\pi A}(M_X^2)}{d^2 b_A}\bigg|_{Gl} &= \left[1 - e^{-\frac{1}{2}\sigma_{tot}^{\pi N}T_A(b_A)}\right]^2 \\ &+ \sigma_{el}^{\pi N}T_A(b_A)e^{-\sigma_{in}^{\pi N}T_A(b_A)}, \quad (7)\end{aligned}$$

where the first and second terms correspond to elastic and quasi-elastic scattering respectively.

The difference between the cross sections, equations (4) and (7) is related to inelastic π-A interactions, leading to multi-particle production. Correspondingly, one should modify equation (4) replacing the total by inelastic πA cross section [8, 9],

$$\frac{\sigma_{in}^{\pi A}(M_X^2)}{d^2 b_A}\bigg|_{Gl} = 1 - e^{-\sigma_{in}^{\pi N}T_A(b_A)} \quad (8)$$

B. Gribov corrections: color transparency

It is well known that the Glauber approximation is subject to Gribov inelastic shadowing corrections [6], which are known to make the nuclear matter more transparent for hadrons [7, 8] and affect both factors in (4), suppressing $\sigma_{tot}^{\pi A}$ and increasing $S_{NA}(b_A)$. We calculate the Gribov corrections to all orders of multiple interactions by employing the dipole representation, as is described in [7–10].

Hadron wave function on the light front can be expanded over different Fock states, consisted of parton ensembles with various transverse positions $\vec{r}_i$ of the partons. The interaction cross section of such a hadron is averaged over the Fock states, $\sigma_{tot}^{hp} = \langle \sigma(\vec{r}_i)\rangle_h$, where $\sigma(\vec{r}_i)$ is the cross section of interaction of the partonic ensemble with transverse coordinates $\vec{r}_i$ with the proton target.

Notice that high-energy partonic ensembles are eigenstates of interaction [7], i.e. the parton coordinates $\vec{r}_i$ remain unchanged during the interaction. Therefore the eikonal approximation employed in the Glauber model, Eqs. (5)-(7) should not be used for hadrons, but for their Fock components, and then the whole exponential terms

should be averaged [7, 10]. This corresponds to the following replacements in Eqs. (5)-(7),

$$e^{-\frac{1}{2}\sigma_{tot}^{hN} T_A} = e^{-\frac{1}{2}\langle\sigma(\vec{r}_i)\rangle_h T_A} \Rightarrow \left\langle e^{-\frac{1}{2}\sigma(\vec{r}_i) T_A}\right\rangle_h. \quad (9)$$

The difference between these averaging procedures is exactly the Gribov corrections [7, 10].

The result of averaging in (9) for proton-nucleus interactions was calculated in [9] with a realistic saturated paramentrization of the dipole cross section [12] and the quark-diquark model for the nucleon wave function.

$$\left\langle e^{-\frac{1}{2}\sigma(r_T) T_A}\right\rangle = e^{-\frac{1}{2}\sigma_0 T_A(b)} \sum_{n=0}^{\infty} \frac{[\sigma_0 T_A(b)]^n}{2^n (1 + n\delta) n!}, \quad (10)$$

where

$$\sigma_0(s) = \sigma_{tot}^{pp}(s)\left[1 + \frac{3R_0^2(s)}{8\langle r_{ch}^2\rangle_p}\right]. \quad (11)$$

We use $\langle r_{ch}^2\rangle_p = 0.8\,\text{fm}^2$ [11], and energy dependent saturation radius $R_0(s) = 0.88\,fm\,(s_0/s)^{0.14}$ with $s_0 = 1000\,GeV^2$ [12].

Gluon shadowing corrections, corresponding to the triple-Pomeron term in diffraction, were introduced as well, as is described in [8, 9].

The results of Glauber model calculations, including Gribov corrections, for the partial inclusive cross section of $pAu \to nX$, equation (4), normalized by the $pp \to nX$ cross section, are plotted in figure 2 by the top solid red (RHIC) and top blue dashed (LHC) curves. The two
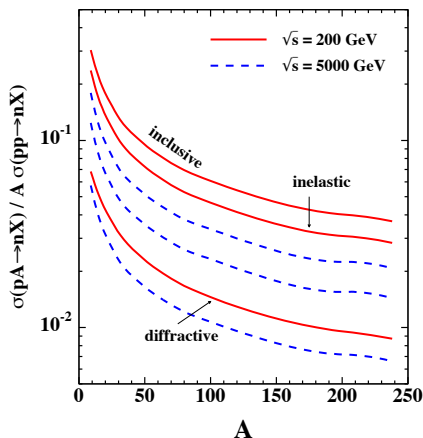

FIG. 2: b_A-integrated cross sections, normalized by the pp cross section of leading neutron production. The solid and dashed curves correspond to both pAu and pPb collisions at $\sqrt{s} = 200\,\text{GeV}$ and $5000\,\text{GeV}$ respectively. The three curves in each set from top to bottom correspond to inclusive, inelastic and diffractive neutron production, respectively.

other lower curves show the cross section of inelastic and diffractive channels. We see that the cross section is very small, what can be understood as a consequence of significant suppression by the factor $S_{NA}(b_A)$ equation (6). Indeed, the impact parameter dependences of the inclusive,

equation (5), and diffractive, equation (7), cross sections of neutron production, are depicted in figure 3. One can
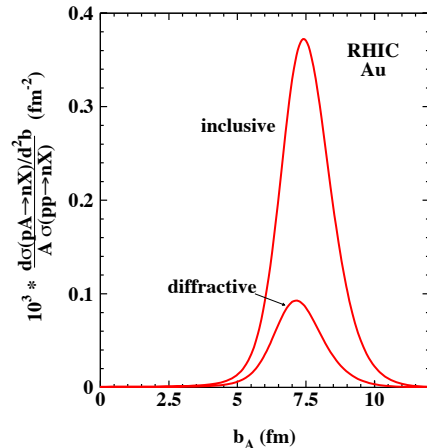

FIG. 3: Partial cross sections for inclusive (upper curve) and diffractive (bottom curve) neutron production in pAu collisions at $\sqrt{s} = 200\,\text{GeV}$ and $z = 0.75$.

see that neutrons are produced from the very periphery of the nucleus, this is why the b_A-integrated cross section is so small. Correspondingly, the ratio shown in figure 2 is falling for heavy nuclei as $A^{-2/3}$.

IV. SINGLE-SPIN ASYMMETRY

A. A_N in polarized $pp \to nX$

Both terms in the amplitude equation (3) have the same phase factor, $\eta_\pi(t) = i - ctg\,[\pi\alpha_\pi(t)/2]$. Therefore, in spite of the presence of both spin-flip and non-flip amplitudes, no single-spin asymmetry associated with pion exchange is possible in the Born approximation. Even the inclusion of absorptive corrections leave the spin effects miserably small [13, 14] compared to data [15, 16].

A plausible candidate to generate a sizeable spin asymmetry at high energies is a_1 meson exchange, since a_1 can be produced by pions diffractively. However, this axial-vector resonance is hardly visible in diffractive channels $\pi + p \to 3\pi + p$, which are dominated by $\pi\rho$ in the 1^+S wave. The $\pi\rho$ invariant mass distribution forms a pronounced narrow peak at $M_{\pi\rho} \approx m_{a_1}$ (due to the Deck effect [17]). Although in the dispersion relation for the amplitude this channel corresponds to a cut, it can be replaced with good accuracy by an effective pole $\tilde{a}_1$ [14, 18]. In the crossed channel, $\pi\rho$ exchange corresponds to a Regge cut, with known intercept and slope of the Regge trajectory [14].

The expression for the single-spin asymmetry arising

from π-$\tilde{a}_1$ interference has the form [14],

$$A_N^{(\pi-\tilde{a}_1)}(q_T, z) = q_T \, \frac{4m_N \, q_L}{|t|^{3/2}} \, (1-z)^{\alpha_\pi(t) - \alpha_{\tilde{a}_1}(t)} \quad (12)$$

$$\times \, \frac{\text{Im} \, \eta_\pi^*(t) \, \eta_{\tilde{a}_1}(t)}{|\eta_\pi(t)|^2} \left(\frac{d\sigma_{\pi p \to \tilde{a}_1 p}(M_X^2)/dt|_{t=0}}{d\sigma_{\pi p \to \pi p}(M_X^2)/dt|_{t=0}} \right)^{1/2} \frac{g_{\tilde{a}_1^+ pn}}{g_{\pi^+ pn}}.$$

The trajectory of the $\pi\rho$ Regge cut and the phase factor $\eta_{\tilde{a}_1}(t)$ are known from Regge phenomenology. The $\tilde{a}_1 NN$ coupling was evaluated in [14], based on PCAC and the second Weinberg sum rule, where the spectral functions of the vector and axial currents are represented by the ρ and the effective $\tilde{a}_1$ poles respectively. This leads to the following relations between the couplings,

$$\frac{g_{\tilde{a}_1 NN}}{g_{\pi NN}} = \frac{m_{\tilde{a}_1}^2 \, f_\pi}{2m_N \, f_\rho} \approx \frac{1}{2}, \quad (13)$$

where $f_\pi = 0.93 m_\pi$ is the pion decay coupling; $f_\rho = \sqrt{2} m_\rho^2 / \gamma_\rho$, and γ_ρ is the universal coupling, $\gamma_\rho^2 / 4\pi = 2.4$.

The parameter-free calculations of A_N in $pp \to nX$ [14] agree well with the PHENIX data [15, 16].

B. A_N in polarized $pA \to nX$

The single-spin asymmetry on a nuclear target due to π-$\tilde{a}_1$ interference can be calculated with a modified equation (12), in which one should replace

$$\frac{d\sigma_{\pi p \to \tilde{a}_1 p}(M_X^2)/dt|_{t=0}}{d\sigma_{\pi p \to \pi p}(M_X^2)/dt|_{t=0}} \Rightarrow \frac{d\sigma_{\pi A \to \tilde{a}_1 A}(M_X^2)/dt|_{t=0}}{d\sigma_{\pi A \to \pi A}(M_X^2)/dt|_{t=0}} \quad (14)$$

This replacement leads to the single-spin asymmetry, which can be presented in the form,

$$A_N^{pA \to nX} = A_N^{pp \to nX} \times \frac{R_1}{R_2} \, R_3. \quad (15)$$

Factor R_1 in accordance with (12) and (14) is the nuclear modification factor for the forward amplitude of $\pi A \to \tilde{a}_1 A$ coherent diffractive transition. In the Glauber approximation it has the form,

$$R_1 = \int d^2 b_A \int_{-\infty}^{\infty} d\zeta \, \rho_A(b_A, \zeta)$$

$$\times \, \exp\left[-\frac{1}{2} \sigma_{tot}^{\pi N} T_-(b_A, \zeta) - \frac{1}{2} \sigma_{tot}^{\tilde{a}_1 N} T_+(b_A, \zeta) \right], (16)$$

where $T_-(b_A, \zeta) = \int_{-\infty}^{\zeta} d\zeta' \rho_A(b_A, \zeta')$ and $T_+(b_A, \zeta) = T_A(b_A) - T_-(b_A, \zeta)$.

Integrating over ζ analytically, we arrive at,

$$R_1 = \frac{1}{\Delta\sigma} \int d^2 b_A \, e^{-\frac{1}{2}\sigma_{tot}^{\pi p} T_A(b_A)}$$

$$\times \left[1 - e^{-\frac{1}{2}\Delta\sigma T_A(b_A)} \right] e^{-\frac{1}{2}\sigma_{tot}^{pp} T_A(b_A)}, \quad (17)$$

where $\Delta\sigma = \sigma_{tot}^{\tilde{a}_1 N} - \sigma_{tot}^{\pi N}$. As was mentioned above and motivated in detail in [14, 18, 19], diffractive production of a_1 axial-vector meson is a very weak signal compared with ρ-π production, which form a rather narrow peak in the invariant mass distribution. Therefore with a good accuracy $\sigma_{tot}^{\tilde{a}_1 N} = \sigma_{tot}^{\rho N} + \sigma_{tot}^{\pi N}$, and $\Delta\sigma = \sigma_{tot}^{\rho N}$. Data for photoproduction of ρ meson on nuclei agree with $\sigma_{tot}^{\rho N} \approx \sigma_{tot}^{\pi N}$, so we fix $\Delta\sigma$ at this value.

Nuclear modification, corresponding to the denominator of equation (14) is determined by Eqs. (4) - (6) and has the form,

$$R_2 = \frac{2}{\sigma_{tot}^{\pi p}} \int d^2 b_A \left[1 - e^{-\frac{1}{2}\sigma_{tot}^{\pi p} T_A(b_A)} \right] e^{-\frac{1}{2}\sigma_{tot}^{pp} T_A(b_A)}. (18)$$

The factor R_3 depends on how the measurements were done. If the BBC are fired, a proper estimate would be $R_3 = \sigma_{tot}^{\pi A} / \sigma_{in}^{\pi A}$. Otherwise, if the BBC are switched off (inclusive neutron productions), we fix $R_3 = 1$. The results corresponding to these two choices are plotted in figure 4, by solid and dotted curves respectively. All data
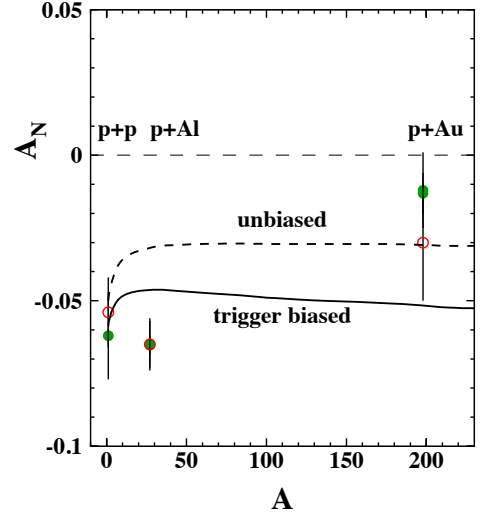

FIG. 4: A_N in polarized $pA \to nX$ vs A at $\sqrt{s} = 200 \, \text{GeV}$, $\langle q_T \rangle = 0.115 \, \text{GeV}$ and $\langle z \rangle = 0.75$. Full and open data points correspond to events with either both BBCs fired, or only one of them fired in the nuclear direction, respectively [20–22]. An attempt to model these two classes of events is presented by solid and dashed curves (see text).

points correspond to events with BBC fired. However full green and open red points correspond to events with either both BBCs fired, or only one of them in the nuclear direction, respectively [20–22].

The difference between these two results reflects the uncertainly in the physical interpretation of events with fired of vetoed BBCs. This can be improved by applying a detailed Monte-Carlo modelling. Nevertheless, the results of our calculations, presented in figure 4, reproduce reasonably well experimental data [20–22].

A remarkable feature of the single-spin asymmetry A_N of neutrons produced on nuclear targets is a very weak

A-dependence, seen both in the data and our calculations. The reason can be easily understood. All A-dependence of the asymmetry A_N is contained in the factors R_1 and R_2 in equation (15). It turns out that the strong nuclear absorption factor $S_{NA}(b_A)$, equation (6), contained in both equations (17) and (18), push neutron production to the very periphery of the nucleus. This is demonstrated by the b_A-unintegrated factors $R_1(b_A)$ and $R_2(b_A)$, plotted in figure 5 for gold at $\sqrt{s} = 200\,\text{GeV}$. Due to the observed similarity of A-dependences of R_1
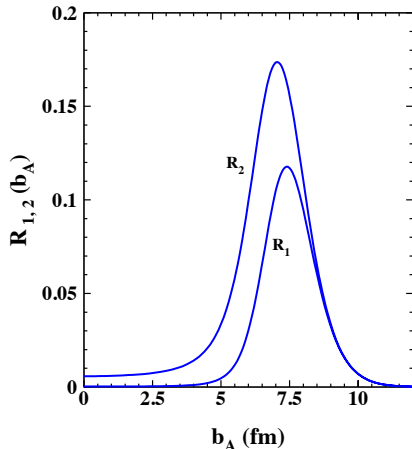

FIG. 5: Partial cross sections for inclusive (upper curve) and diffractive (bottom curve) neutron production in pAu collisions at $\sqrt{s} = 200\,\text{GeV}$.

and R_2, $\propto A^{1/3}$, they mostly cancel in (15), resulting in nearly A-independent single-spin asymmetry of neutrons.

V. SUMMARY

The previously developed methods of calculation of the cross section of leading neutron production in pp collisions, are extended to nuclear targets. The nuclear absorptive corrections, calculated in the Glauber-Gribov approach, are so strong that push the partial cross sections of leading neutron production to the very periphery of the nucleus. As a result, the A-dependences of inclusive and diffractive neutron production turn out to be similar, $\sim A^{1/3}$.

The mechanism of π-a_1 interference, which successfully explains the observed single-spin asymmetry in polarized reaction $pp \to nX$, is extended to collisions of polarized protons with nuclei. Corrected for nuclear effects, it explains quite well the observed asymmetry A_N in inelastic events, when the nucleus violently breaks up [20–22]. However, the large value and opposite sign of A_N observed in the diffractive sample, still remains a challenge.

Acknowledgments

[1] B. Z. Kopeliovich, I. K. Potashnikova, I. Schmidt and J. Soffer, "Damping of forward neutrons in pp collisions," Phys. Rev. D **78**, 014031 (2008).

[2] H. E. Haber and G. L. Kane, "The Search for the a1 Meson," Nucl. Phys. B **129**, 429 (1977).

[3] B. Kopeliovich, B. Povh and I. Potashnikova, "Deep-inelastic scattering on the pion cloud of the proton", Z. Phys. C **73**, 125 (1996).

[4] B. Z. Kopeliovich, I. K. Potashnikova, B. Povh and I. Schmidt, "Pion structure function at small x from DIS data," Phys. Rev. D **85**, 114025 (2012).

[5] B. Z. Kopeliovich, H. J. Pirner, I. K. Potashnikova, K. Reygers and I. Schmidt, "Pion-pion cross section from proton-proton collisions at the LHC," Phys. Rev. D **91**, 054030 (2015).

[6] V. N. Gribov, "Glauber Corrections And The Interaction Between High-Energy Hadrons And Nuclei," *Sov. Phys. JETP* **29**, 483 (1969) [Zh. Eksp. Teor. Fiz. **56**, 892 (1969)].

[7] B. Z. Kopeliovich, L. I. Lapidus and A. B. Zamolodchikov, "Dynamics of Color in Hadron Diffraction on Nuclei," JETP Lett. **33**, 595 (1981) [Pisma Zh. Eksp. Teor. Fiz. **33**, 612 (1981)].

[8] B. Z. Kopeliovich, "Transparent nuclei and deuteron-gold collisions at relativistic energies", Phys. Rev. C **68**, 044906 (2003).

[9] B. Z. Kopeliovich, I. K. Potashnikova and I. Schmidt, "Large Rapidity Gap Processes in Proton-Nucleus Collisions", Phys. Rev. C **73**, 034901 (2006).

[10] B. Z. Kopeliovich, "Gribov inelastic shadowing in the dipole representation," Int. J. Mod. Phys. A **31**, no. 28n29, 1645021 (2016).

[11] R. Rosenfelder, "Coulomb corrections to elastic electron proton scattering and the proton charge radius", Phys. Lett. B **479**, 381 (2000).

[12] B. Z. Kopeliovich, A. Schäfer and A. V. Tarasov, "Non-perturbative effects in gluon radiation and photoproduction of quark pairs," Phys. Rev. D **62**, 054022 (2000).

[13] B. Z. Kopeliovich, I. K. Potashnikova, I. Schmidt and J. Soffer, "Leading neutrons from polarized pp collisions," AIP Conf. Proc. **1056**, 199 (2008) [arXiv:0807.1449 [hep-ph]].

[14] B. Z. Kopeliovich, I. K. Potashnikova, I. Schmidt and J. Soffer, "Single transverse spin asymmetry of forward neutrons," Phys. Rev. D **84**, 114012 (2011).

[15] A. Adare *et al.* [PHENIX Collaboration], "Inclusive cross section and single transverse spin asymmetry for very forward neutron production in polarized pp collisions at

$\sqrt{s} = 200\,\mathrm{GeV}$", Phys. Rev. D **88**, 032006 (2013).

[16] Y. Goto [PHENIX Collaboration], "Inclusive cross section and single transverse-spin asymmetry of very forward neutron production at PHENIX," Phys. Part. Nucl. **45**, 79 (2014).

[17] R. T. Deck, "Kinematical interpretation of the first pi - rho resonance," Phys. Rev. Lett. **13**, 169 (1964).

[18] A. A. Belkov and B. Z. Kopeliovich, "Adler Relation and Neutrino Production of Single Hadrons," Sov. J. Nucl. Phys. **46**, 499 (1987) [Yad. Fiz. **46**, 874 (1987)].

[19] B. Z. Kopeliovich, I. K. Potashnikova, I. Schmidt and M. Siddikov, "Breakdown of PCAC in diffractive neutrino interactions," Phys. Rev. C **84**, 024608 (2011).

[20] A. Bazilevsky, "PHENIX Spin Program: achievements and recent results", a talk presented at the 6th International Workshop on High Energy Physics in the LHC Era, 6-12 January 2016, Valparaiso, Chile.

[21] I. Nakagawa, "The First Asymmetry Measurements in High-Energy Polarized Proton-Nucleus Collision at PHENIX-RHIC", a talk presented at the 5th International Conference on New Frontiers in Physics, 6-14 July 2016, Crete, Greece.

[22] A. Bazilevsky, "PHENIX recent results from polarized pp and pA collisions", a talk presented at the conference Diffraction 2016, 2-8 September, 2015, Catania, Sicily.